Mechanics & Industry **22**, 49 (2021)

https://doi.org/10.1051/meca/2021050

Mechanics & Industry

Available online at:
www.mechanics-industry.org

REGULAR ARTICLE

OPEN ACCESS

Hybrid skyhook mass damper

Simon Chesné*

Université de Lyon, CNRS INSA-Lyon, LaMCoS UMR5259, 69621 Villeurbanne, France

Received: 11 August 2021 / Accepted: 16 November 2021

Abstract. The objective of this study is to increase the efficiency of an initial passive Tuned Mass Damper (TMD) by adding an active control unit. A critical issue in many engineering domains is the design of fail-safe active systems. The proposed hybrid system aims to address this issue and realizes the said objective. It emulates the behavior of a skyhook damper parallel to a passive TMD. Skyhook dampers acts like viscous dampers connected to the ground, reducing the vibration amplitudes without any overshoot. It can be difficult to design a specific control law to obtain a desired dynamical behavior. The paper presents two ways to understand and design the hyperstable control law for Hybrid Mass Damper (HMD) (also called Active TMD), using the power flow formulation or the mechanical impedance analysis. These approaches are illustrated through the synthesis of this hybrid device and the emulation of the Skyhook damper. It is shown that a well-designed control law for this kind of system may result in high damping performance, ensuring stability and a fail-safe behavior. In addition, the amplitude of the primary system's response is reduced over the entire frequency range which is not the case for the usual active or hybrid systems. Robustness is analyzed and compared to that of the classical active mass damper, and an experimental set up validates the proposed hybrid system.

Keywords: Tuned mass samper / active vibration control / skyhook damper / velocity feedback / electromagnetic damper

1 Introduction

Tuned Mass Dampers (TMDs) are a very well known device that reduces vibration amplitude on targeted modes. For decades, many successful applications have proven their efficiency and robustness, using the usual equal peak design proposed by Den Hartog [1,2]. The closed form of the optimization's solution has been established recently by Asami [3]. Nevertheless, amplitude reduction on the targeted mode is limited by the oscillating mass of the device. To overcome this problem, many authors have proposed to modify the initial passive system, by introducing non linearities [4,5] or by adding an active system to the passive TMD. Due to the resulting large stroke, such systems are usually designed using a voice coil actuator as a hybrid TMD. However, even if the performance is drastically increased, the stability limit remains a critical issue. Performance and stability are linked to the resulting power flows in the system [6]. The impedance or mobility analysis helps authors understand these flows and tune the control to ensure the stability of the proposed active systems [7–9]. To improve the performance, others approaches tried to modify the dynamical behavior of the TMD by reducing its resonance frequency of the oscillator. In this way it can be used as an Active Mass Damper (AMD) through a dual loop configuration [10]. Few of these configurations are hyperstable. In many cases, the stability is ensured by more complex controllers necessitating feedback loops using many measurements, such as the backstepping control approach [11], H_∞ robust control [12], zero/pole-assignment [13], and fuzzy neural network algorithm [14]. Hybridization can also be used to reduce the power consumption of an active controller [15], or embedded on a rotating machine, can be fully autonomous [16]. Recently, a control law, acting as a phase compensator, has been proposed to get this device unconditionally stable [17,18].

Most of these approaches drastically reduce the system's response at the desired frequency but increase the vibration amplitude around the initial resonance frequency, as a passive TMD does. One passive way to reduce the amplitude in the whole frequency range is to use a Sky-Hook Damper. Skyhook damping requires that a viscous damper be connected to the ground, which is not physically possible for embedded applications. Many purely active sustems try to synthetize the dynamical behavior of ashyhook damper in order to increase the damping of the primary structure. It can easily be realized using an

* e-mail: simon.chesne@insa-lyon.fr

AMD and a direct velocity feedback [19–21], but the system is not hyperstable and the fail-safe behavior is not certain as the actuator is not tuned on the main resonance as for a TMD. Recently, [22] proposed to combine a dynamic vibration absorber (DVA) with an electromagnetic shunt damper, showing that this association allows damping the resonances while keeping the strict antiresonance created by the DVA. A semi-active controller can also be a good candidate for hybridization [23], to reduce the energy demand again. Many realizations and applications are proposed [24,25]. Hybridization can also be extended to isolation problem when using an inertial isolator and feedforward architecture [26]. As underlined in [17] or [25], the hybrid system needs to be carefully analyzed in terms of stability or required power. In conclusion, it appears that active or hybrid techniques provide us with a very flexible tool to reduce vibration depending on the available device and the defined objectives.

This paper presents a new hybrid device associating a single feedback loop and a TMD used as actuator. It also shows how to use power flow formulation and equivalent mechanical impedance to design a specific control law for this HMD. Due to the existence of a full mechanical analogy, the resulting hybrid device is theoretically hyperstable and provides infinite gain margins. The device also presents a so-called fail-safe behavior because the chosen actuator parameters are equal to those of an optimal passive TMD. The resulting system emulates a Skyhook damper parallel to this optimal TMD. After the theoretical presentation of the hybrid device on a simple structure, the paper illustrates how to design this kind of control law. Then, the resulting stability, the performance, and the robustness are analyzed through numerical simulations. All these aspects are also compared with a standard AMD (which is purely active and not fail-safe) that provides the usual skyhook damping. Finally, experimental results validate the proposed hybrid device and its performance. It clearly shows the main advantages of such a device: performance, stability and vibration reduction over the entire frequency band of interest.

2 Mathematical model

This section illustrates the principle of the HMD and its equivalent full mechanical analogy in the case developed in this paper.

A typical linear hybrid system is shown in Figure 1a. It is composed of a primary system (index 1) associated with a TMD (index 2). Hybridization is done by adding an active force driven by a control unit. The disturbance on the primary system can come from the ground (X_0) or from an external force on the primary structure (F_1). Control performance is similar regardless of the disturbance. In the following, F_1 will be mainly used. Figure 1b represents the equivalent mechanical system when the controller is adequately tuned to synthesize a skyhook damper (as shown in the following parts). It results in the association of an optimal passive TMD with a synthesized skyhook damper.

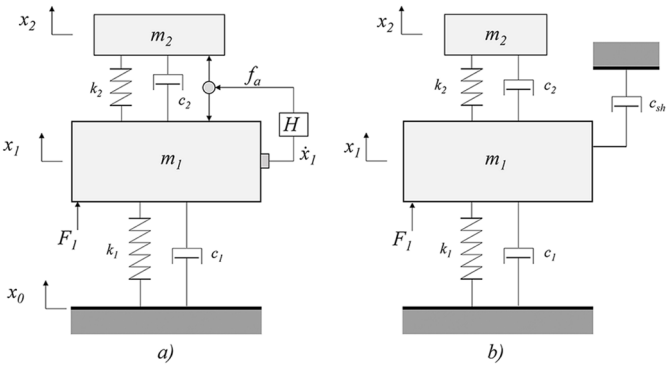

Fig. 1. Schematics of the control unit model used in the simulations. a) Hybrid Tuned Mass Damper, b) Passive system (Tuned Mass Damper and Skyhook Damper).

The governing equations of motion are written in the Laplace domain as follows:

$$s^2 m_1 X_1 = (k_2 + sc_2)(X_2 - X_1) - F_a + F_1 + (k_1 + sc_1)(X_0 - X_1) \quad (1)$$

$$s^2 m_2 X_2 = (k_2 + sc_2)(X_1 - X_2) + F_a \quad (2)$$

where s is the Laplace variable, m_1 and m_2 are the masses, X_1 and X_2 are their displacements in the Laplace domain, k_1 and k_2 are the stiffness values, and c_1 and c_2 are the mechanical damping values of the primary system and the TMD. c_{sh} is the damping value of the equivalent mechanical skyhook damper. X_0 represents the ground motion, F_1 the external disturbance force applied on the primary system, and F_a the control force. The TMD is designed using the equal peak design rules [2]:

$$\omega_2 = \frac{k_2}{m_2} = \frac{k_1}{m_1} * \nu \quad (3)$$

with $\nu = 1/(1+\mu)$ and

$$\xi_2 = \frac{c_2}{2\sqrt{k_2 m_2}} = \sqrt{\frac{3\mu}{8(1+\mu)}} \quad (4)$$

where ω_2 is the natural frequency of the TMD, ξ_2 is its damping ratio and μ is the mass ratio (m_2/m_1). For this study, μ is set at 1%, which is representative of the concerned applications. The controller H, generating the equivalent mechanical behavior illustrated in Figure 1b, will be defined in the next part. Based on the measurement of the primary system's velocity (as a classical velocity feedback), the resulting active force can be written as follows:

$$F_a = sHX_1 \quad (5)$$

3 Active damping: Skyhook synthesis

In this section, the idea is to use a simple formulation in terms of power flow to design the appropriate control law. For the analysis developed here, only active damping is conside where the actuator force is fed by a specific velocity feedback. For sake of simplicity we consider the system without internal mechanical damping ($c_1 = c_2 = 0$). As explained previously, to ensure the fail-safe behaviour, the design of the actuator is based on the parameter of a TMD. Consequently, the usual control law of the Direct Velocity Feedback presents poor stability margins [17,18] and has to be modified.

3.1 Power flow formulation

The well-known energy conservation principle, satisfied by any physical systems, explained that the variation of stored energy is the sum of external power input and internal power generation [27].

As the internal mechanical damping values (c_1 and c_2) are set to zero, the internal power generation mechanisms are only linked to the power flow generated by the actuator driven by the controller and its control law $H(s)$. Considering perfect transducers, the function $G(s)$ that represents this dissipating mechanism can be written in the Laplace domain as follows:

$$G(s) = -F_a s(X_1 - X_2) \tag{6}$$

Using equation (5), it becomes:

$$G(s) = (sX_1)^2 H(s)\left(1 - \frac{X_2}{X_1}\right) \tag{7}$$

In terms of stability, the resulting system is passive (hyperstable) if [27]

$$Re[G(s)] > 0 \tag{8}$$

where $Re[\cdot]$ denotes the real part of the function. This condition means that the system is purely dissipative.

On the other hand, one can easily show that the power dissipated by a mechanical Skyhook Damper (as represented in Figure 1 with a damping value of c_{sh}) is:

$$G(s) = (sX_1)^2 c_{sh} \tag{9}$$

Consequently $H(s)$ can be designed in interaction with the TMD's dynamics to ensure stability ($Re[G(s)] > 0$) and the Skyhook Damper emulation. To obtain an equivalence between equations (7) and (9), one can simply define $H(s)$ as:

$$H(s) = g\left(1 - \frac{X_2}{X_1}\right)^{-1} \tag{10}$$

where g is the gain of the feedback loop and will be equal to synthesized skyhook damping c_{sh}. Using equations (1) and (2), one can rewrite the previous equation and observe

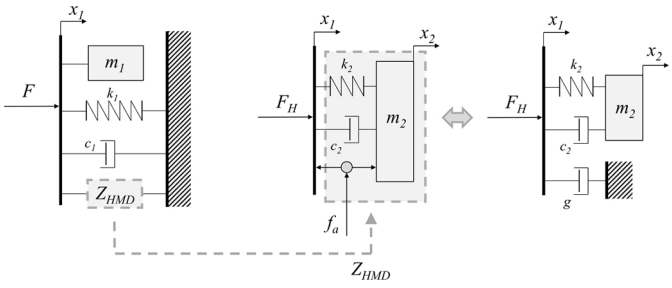

Fig. 2. (a) Parallel representation of the global system, (b) Schematic of the hybrid device and (c) its equivalent mechanical model.

that $H(s)$ depends only on the TMD parameters, not on the primary structure parameters:

$$\begin{aligned} H(s) &= g\left(1 + \frac{c_2}{m_2 s} + \frac{\omega_2^2}{s^2}\right) \\ &= \frac{g}{s^2}\left(s^2 + sc_2/m_2 + \omega_2^2\right) \end{aligned} \tag{11}$$

With this control law, equation (7) verifies condition (8).

3.2 Mechanical impedance analysis

In practice, the simple control law defined in equation (11) will correct TMD's dynamical behavior to generate a virtual skyhook damper attached to the ground. This fact is noticeable because it provides absolute damping on the primary structure, even for embedded applications. The following gives another overview of the approach in terms of mechanical impedance.

On a single degree of freedom, the mechanical impedance Z in Laplace domain can be defined as the ratio between the applied force and the resulting velocity:

$$Z = F/(sX) \tag{12}$$

Figure 2a shows a representation of the global system, illustrating the fact that the impedance of the primary structure is in parallel with that of the HMD. Figure 2b isolates the HMD. One can compute the resulting force F_H generated by the hybrid device at its interface as follows:

$$F_H = (k_2 + sc_2)(X_1 - X_2) + F_a \tag{13}$$

By using equation (2), one can write:

$$F_H = \frac{s^2 m_2(k_2 + sc_2)}{s^2 m_2 + sc_2 + k_2} X_1 + \frac{s^2 m_2}{s^2 m_2 + sc_2 + k_2} HsX_1 \tag{14}$$

Then, by introducing the proposed control law $H(s)$ defined in equation (11), the mechanical impedance of the proposed device is:

$$Z_{HMD} = \frac{F_H}{sX_1} = \frac{sm_2(k_2 + sc_2)}{s^2 m_2 + sc_2 + k_2} + g \tag{15}$$

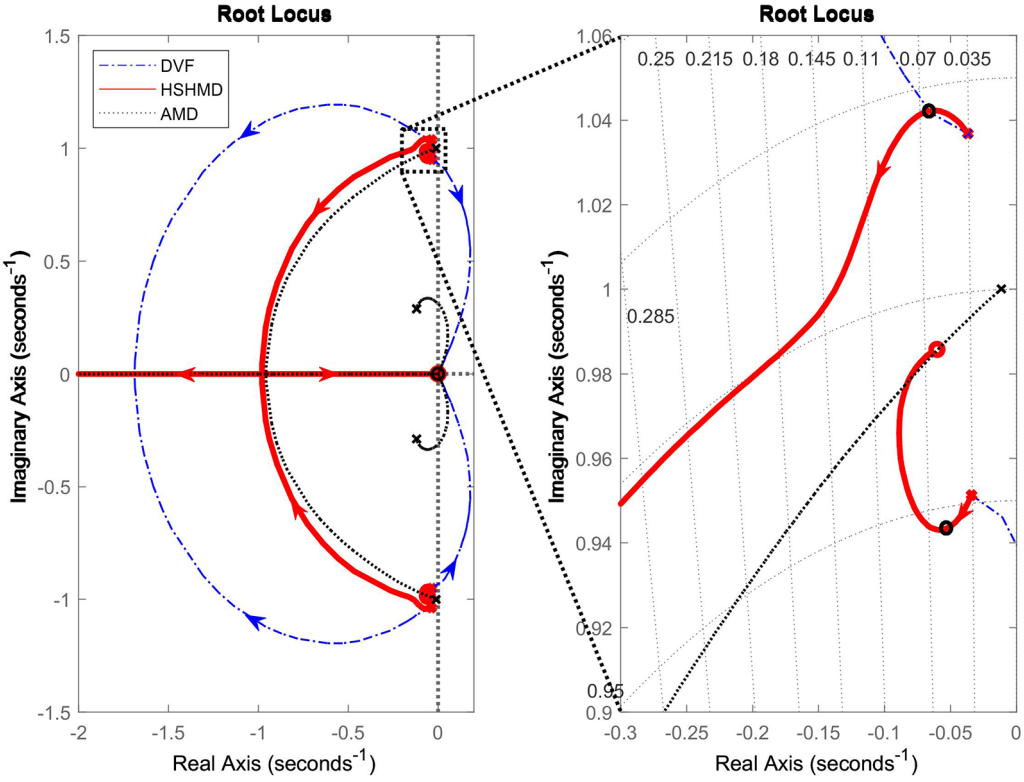

Fig. 3. Root locus of hybrid devices. Blue: Direct Velocity Feedback. Red: Hybrid SkyHook Mass Damper. Black: Active Mass Damper.

$$= Z_{TMD} + Z_{SkyHook} \tag{16}$$

One can clearly identify the terms representing the mechanical impedance of a purely passive TMD (Z_{TMD}) in parallel to skyhook damper with a damping value g ($= Z_{SkyHook}$). The resulting mechanical system is illustrated in Figure 2c.

This section shows that, knowing the actuator's dynamical behavior, and the desired impedance one can easily find a control law using this equivalent impedance analysis. Associated with the power flow formulation, it is a useful tool to understand the stability of the control system.

4 Stability analysis

Considering the system shown in Figure 1, the proposed hybrid device (Hybrid SkyHook Mass Damper: HSHMD), was compared to two classical devices in term of stability. The first was a classical Direct Velocity Feedback (DVF) using the TMD as actuator. The second was an Active Mass Damper (AMD), which is a DVF law applied on an inertial actuator tuned 2 octave lower than the TMD. For the main structure, the mechanical parameters used in these simulations were: $m_1 = 1\,\text{kg}$, $k_1 = 1\,\text{N/m}$ and $\xi_1 = 1\%$. The added mass was 1% of the mass of the main structure, $m_2 = 0.01 * m_1$. These normalized parameters were chosen to be consistent with many transportation and aeronautical applications.

The corresponding root locus and a zoom around the modes of interest are shown in Figure 3.

The root locus of the AMD (black dotted line) shows two loops: a small loop at low frequency associated with the dynamics of the actuator, and a bigger one linked to the mode to damp. This kind of active device is very efficient to damp the main mode of the host structure. However, in case of failure, the system is no longer damped because the AMD parameters are not tuned adequately. The fail-safe behavior is no longer certain. Moreover, for high gains, the system is not stable at low frequency.

To obtain a fail-safe system, the mechanical parameters k_2 and ξ_2 were chosen according Den Hartog's rules [28]. If applying a DVF to this system (blue dash-dotted line), the lower frequency pole goes immediately in the right half-plane, leading to instability.

Now if the control law defined in equation (11) is used on the tuned device, we obtain the root locus plotted in red in Figure 3. We can see that the poles stay in the left half-plane of the plot whatever the gain is. This illustrates the infinite gain margin characterizing the hyperstability. For very high gains, it can be seen that the pole linked to the main structure becomes real and the pole linked to the actuator moves to a location representative of the pole of the isolated passive TMD.

The above-mentioned behaviors and limits can also be observed on the open-loop transfer functions of these hybrid devices (Fig. 4). On the bode representation, the phase of the HSHMD always stays far from the $+/-180\,\text{deg}$ limits. The Nyquist representation clearly

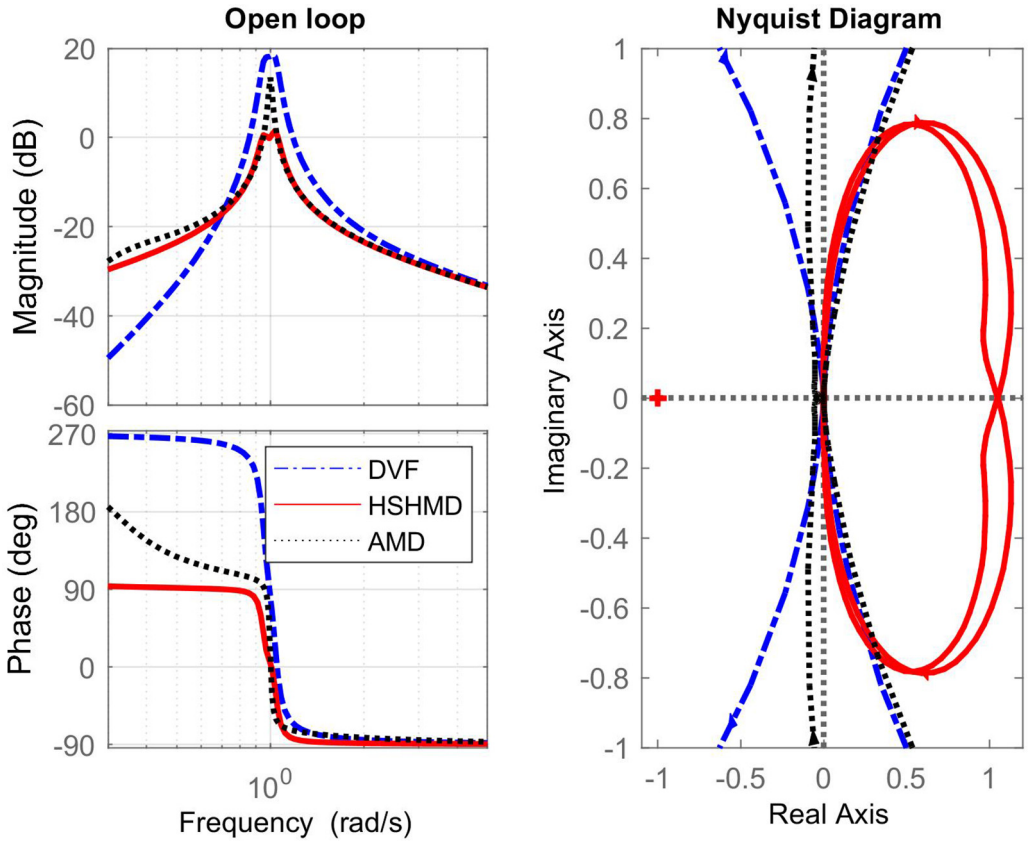

Fig. 4. Bode and Nyquist open loop transfer functions. Blue: Direct Velocity Feedback. Red: Hybrid SkyHook Mass Damper. Black: Active Mass Damper.

shows the hypertability property of the HSHMD. For instance, for the open loop frequency response function with the proposed control law, the circle of the resonance is rotated clockwise into the real-positive quadrants. This indicates that the closed feedback loop is unconditionally stable.

In addition, we can understand that because of the full analogy with a mechanical network presented in the previous section, the stability of the active system is guaranteed if we consider idealized force sensors and actuators.

5 Performance

In the following, the HSHMD is compared with the passive TMD and the purely active AMD. The DVF control law applied on a TMD is no longer considered due to its lack of stability. Each of these devices is considered to be mounted alternatively on the system shown in Figure 1. As these devices are clearly different, their parameters have been chosen arbitrarily. The damping of the initial system is 1%, and the poles with a passive TMD present a damping of 3.5%, which is coherent with the mass ratio $\mu = 1\%$. The active control gain of the HSHMD and that of the AMD are both tuned to obtain modes with about 6.5% of damping. For these tuning parameters, the resulting active forces for both configurations, reach the same maximum amplitudes in impulse perturbation.

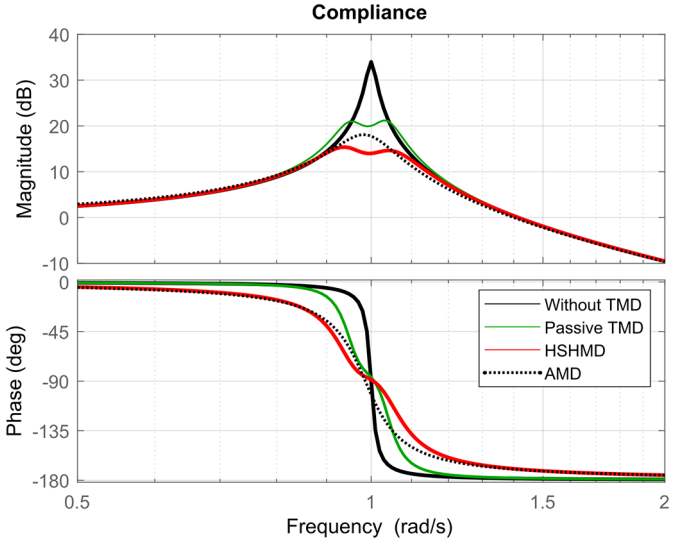

Fig. 5. Frequency Response Functions x_1/F_1 of the closed loop system.

Figure 5 shows the frequency response functions x_1/F_1 for the controlled systems. The black, green, and dotted lines represent the responses of the classical systems used as a reference here. They are the uncontrolled system (black line), the passively controledl system with a

TMD (green line), and the actively controlled system with an AMD (black dotted line). Looking at the red curve (for the HSHMD), we can understand that the proposed hybrid device perfectly combines the passive properties of the TMD (pole duplication) and the synthesis of a skyhook damper as the AMD does (add of an absolute damping).

In [29], it was shown that other classical hybrid systems, present a compromise in their response. An amplitude reduction in a given frequency range, often results in an increase elsewhere. In contrast to these hybrid systems, one can note here for the HSHMD, that the resulting curve is fully under the reference curve of the passive TMD. No overshoot is observed. This is due to the absolute damping introduced by the skyhook damper. This property represents an important gap in the development of future hybrid absorbers.

The final behavior of the hybrid device corresponds exactly to its mechanical analogy illustrated in Figure 2.

6 Practical considerations

Even if the performance previously shown are very attractive, other phenomena have to be considered. It will results in some compromises that have to be anticipated. In the following, the perturbation force F_1 is a white noise with a power spectral density equal to 1.

6.1 Robustness

Because the control law (11) is tuned on the mechanical parameters, one has to investigate the robustness of the system versus a stiffness variation. This type of variation seems to be more relevant to this study.

Both variations on k_1 (main structure) and k_2 (mass damper) are considered. $\Delta(k_i)$ is a multiplicative factor applied to the stiffness k_i. The case $\Delta(k_i) = 1$ represents the reference case of the previous section. Figure 6 illustrates the resulting attenuation in terms of the H_∞ norm.

As expected, the AMD (black dotted line) is not really affected by these variations. It is due to the fact that neither the control law nor the actuator is tuned on the mechanical parameters. The performance of the passive TMD (in green) decreases rapidly for any variations on k_1 or k_2, which corresponds to both cases of the device detuning.

HSHMD (in red) presents a combination of both behaviors. In the case of a k_1 variation, the attenuation is still very high. The control law is still adapted to its actuator, and the synthetic skyhook damper is still very effective. For a k_2 variation, the control law (which is always tuned on the initial parameters) seems less effective, and the system behaves like a detuned TMD.

These observations are coherent with the philosophy of the proposed control law. Indeed it can be seen as a compensator of the dynamical behavior of the TMD to use its mass as a ground reference. The control law is directly linked to the parameters of the device.

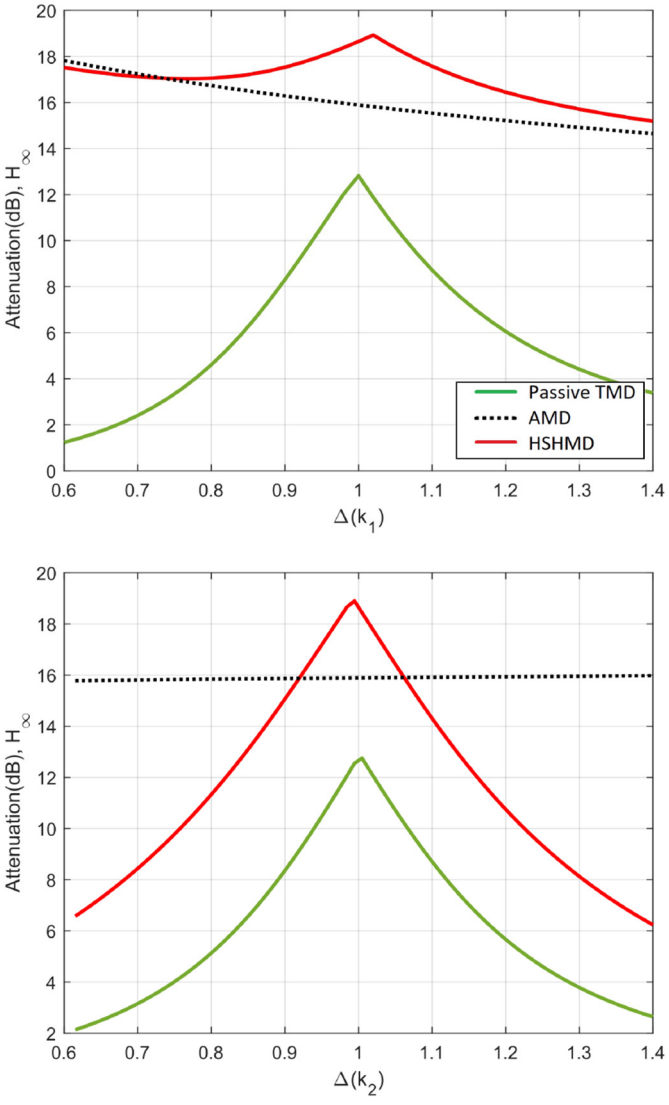

Fig. 6. Evolution of the H_∞ attenuation for (a) a variation on k_1 and (b) a variation on k_2. Green: Passive TMD. Black dotted line: AMD. Red line: HSHMD.

Whatever the case, the resulting stability margins are still very high. The gain margin is always infinite, and the phase margin is reduced from 90 deg (see Fig. 4) to 85 deg in the worst case. Observations on the H_2 norm are very similar and are not presented here. Note that the stiffness variations simulated here are very high $(+/-40\%)$.

6.2 Actuator stroke

The actuator stroke is another point of view from which to analyze the hybrid device. The stroke of a passive TMD is linked to the resulting dissipated energy. In case of the hybrid devices, it is combined with the active force effect. However the stroke can always appear as a practical limitation (available space, stiffness linearity, etc). The stroke spectrum is shown in Figure 7. The stroke is simply assumed to be equal to $(x_2 - x_1)$.

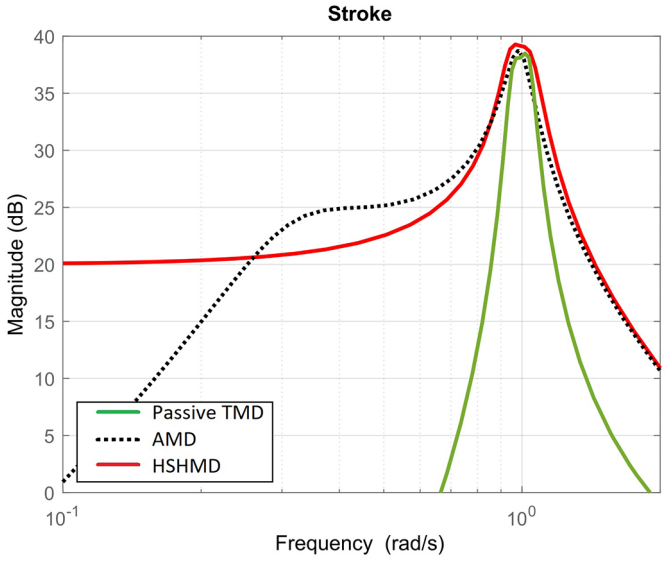

Fig. 7. Stroke comparison depending on the device (Green: Passive TMD. Black dotted line: AMD. Red line: HSHMD).

At the vicinity of the resonant frequency of the primary structure, all the simulated strokes are important. The passive TMD dissipates energy in its dashpot, and the AMD generates high force by using the inertia of its actuator. At these frequencies, the HSHMD presents a slightly higher stroke (+1 dB).

The main drawback can be seen at low frequencies where the effect of the integrator of the control law generates important relative displacements. One can understand that the superior performance of the HSHMD controller is obtained at the cost of a much larger stroke of the device mainly at low frequencies. The last section discusses this point and how to avoid this important theoretical drawback.

6.3 Active force and effective power

Using the previous simulation parameters, the active force and the effective power for AMD and HSHMD are shown in Figure 8. These quantities are extremely important for any practical implementations of the device. Indeed, the transducer (usually electromagnetic) has to generate the active force, and its related amplifier must provide the needed power (usually electrical).

As expected, these two quantities present similar behaviors. Near the resonant frequency, the hybrid device needs less active force and then, less power than the purely active device. Because the actuator of the hybrid device is tuned on this frequency. A small force is necessary to generate high displacements and inertial forces. This property can be of interest to counter harmonic perturbation, as already shown in [10]. Again, one can observe the main drawback of the hybrid system at low frequencies. In fact, the control law generates a high active force and requires a significant effective power, mainly because of the integrators present in the control law.

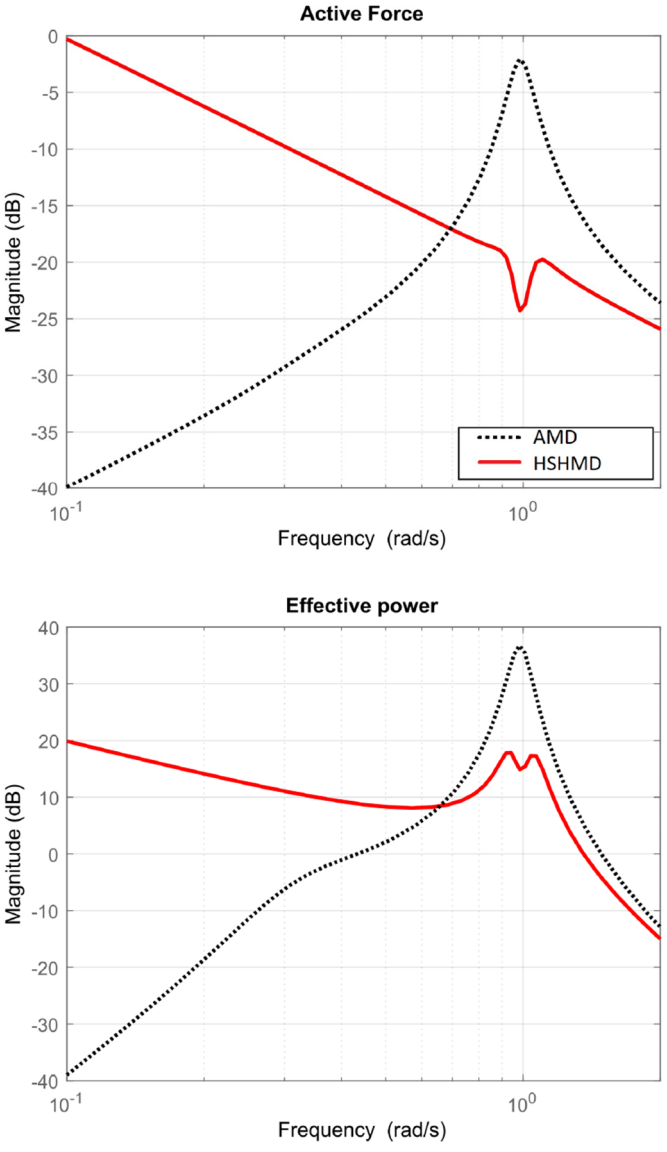

Fig. 8. Comparison of active force and global power consumption (Black dotted line: AMD. Red line: HSHMD).

7 Experimental validation

7.1 Set-up description

The control system and the setup is represented in Figure 9. It is a cantilever steel beam ($58 \times 10 \times 1$ cm). The hybrid device is rigidly mounted on the beam at 48 cm from the base. This electromagnetic system is a Micromega product (ADD-5N), originally designed for active control. This transducer has not been specifically designed or optimized for this application, but its mechanical parameters correspond to those we are looking for in this demonstration. Its moving mass is 160 g. When associated with its current amplifier, its resulting resonant frequency is around 25 Hz, and its internal damping of $\xi_2 = 19\%$. All these parameters have be estimated using the rational fraction form method (RFP) [30] from the

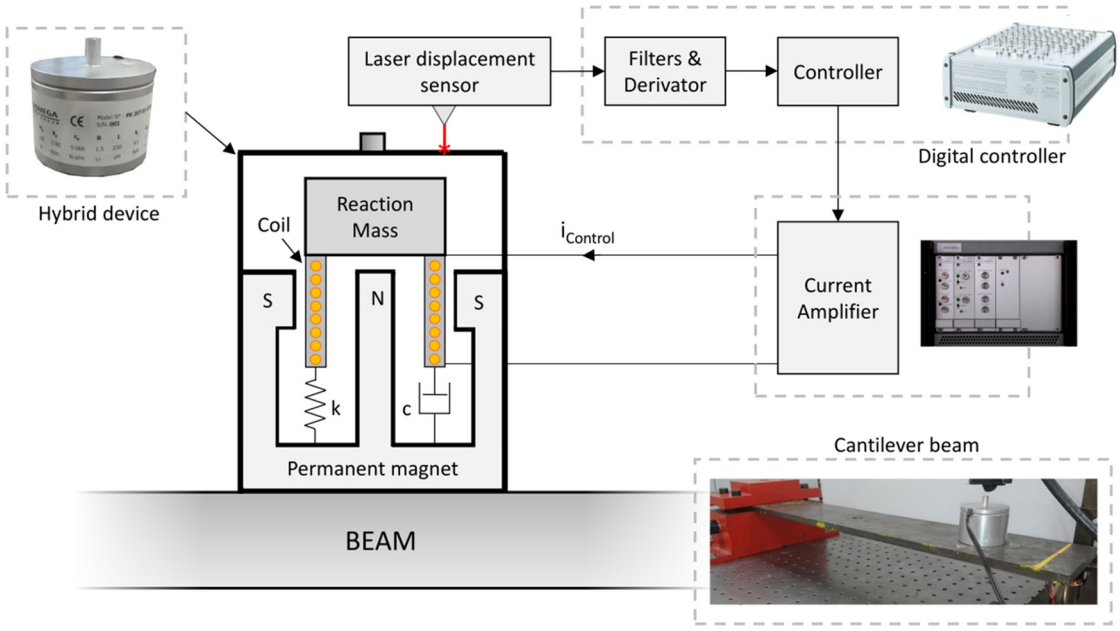

Fig. 9. The control system, its feedback loop, and the experimental setup.

measured transfer functions shown in Figure 10. The passive attenuation observed in Figure 10 is around 18 dB, then the resulting mass ratio μ is estimated at around 8%. A laser displacement sensor is used to measure the displacement at the device location. The resulting velocity used in the control loop can be estimated by derivation.

In this proof of concept, the focus is given to the first bending mode. In practice, neither the resonant frequency nor the damping of the TMD is perfectly tuned to verify the equal peak design as defined by [2]. Nevertheless, as shown in the next section, it doesn't compromise the good performance of the proposed approach. The perturbation is a white noise applied at the free extremity of the beam through an electromagnetic actuator.

7.2 Filters and velocity estimation

Many control systems to increase damping in a structure use a velocity feedback loop. This input usually comes from an accelerometer associated with an integrator. As pointed out in the previous sections, the main drawback of the proposed controller is the presence of integrators in the control law (poles in zero in Eq. (11)). It may enhance the command at low frequencies and then lead to stroke or force saturation effects in the actuator. To avoid these negative effects, two solutions are implemented.

First, a laser displacement sensor is used in the feedback loop. It allows to cancel one integration step in the control loop with the derivative step necessary to estimate the velocity. It then reduces the order of the integrator.

Moreover, a high-pass filter is added in the feedback loop (second-order Chebychev filter at 1 Hz). Theoretically, the introduction of this high pass filter compromises the hyperstability of the proposed control law (no more infinite gain margin). However, in practice, the stability margins are still extremely high, and don't appear as a limitation, as proven in the following.

7.3 Results

The performance of the control device is observed in terms of the displacement response at the actuator location. The white noise feeding the perturbation actuator is used as reference. Figure 10 shows the displacements of the beam without a TMD (gray line), with a passive TMD (green line), and with the HSHMD using different gains in red (continuous line: $g = 60$, dotted line: $g = 180$). The TMD almost verifies the equal peak property. One can observe the effect of the HSHMD device on the first mode. Depending on the gain, it can reach a huge attenuation compared to the passive device. Also, the dynamical amplification of the two resulting modes are almost canceled.

The red curves are always under the green one regardless of the frequency range. This is one of the main particularities and advantages of this HSHMD, which is linked to the synthesis of the skyhook damper.

This property can also be observed in Figure 11. It shows the cumulative sum of the previous frequency response functions. The hybrid system drastically reduces this cumulative sum.

Figure 12 shows the root locations for various values of the gain compared with the simulated root locus. Note that the initial state (passive TMD) represented by the gray cross is experimentally identified. This figure shows a good correlation between a simulated control and an experiment.

The effect of the high-pass filter is negligible and not represented here. Even if the theoretical hyperstability is lost, the resulting gain margin is still very high, around 75 dB. The stability is not the main limitation to increase

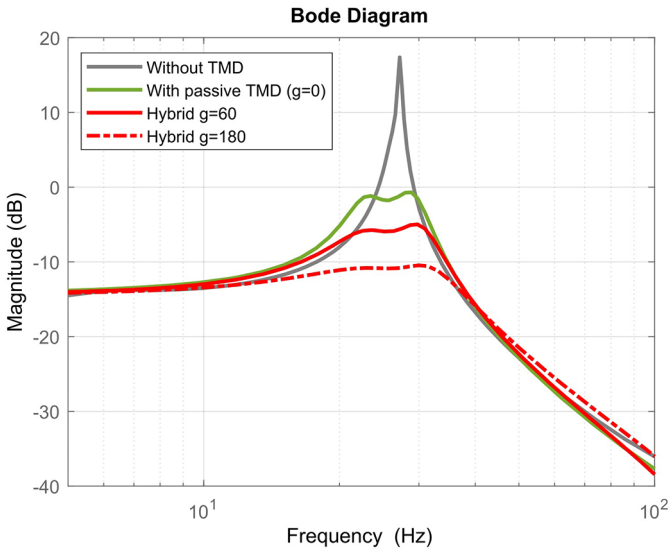

Fig. 10. Frequency response function in term of displacements without TMD (grey line), with passive TMD (green line) and with the HSHMD using different gains in red (Continuous line: $g = 60$, dotted line: $g = 180$).

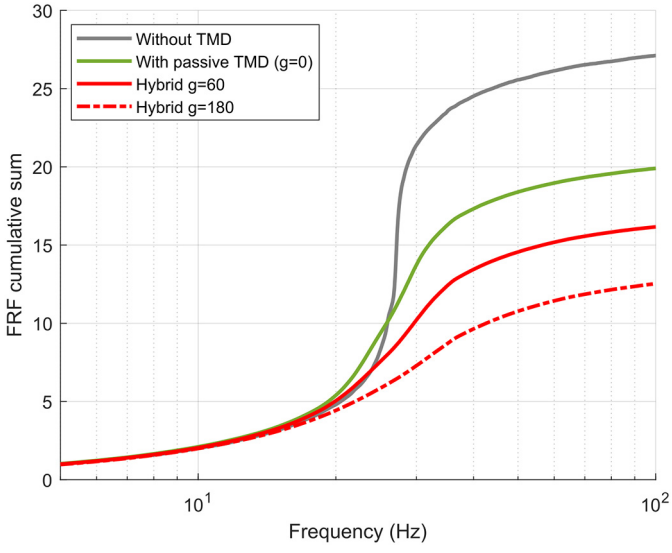

Fig. 11. Cumulative sums of FRF represented in Figure 10.

the controller gain. In this setup, higher gains have not been tested due to the saturation limit of the current amplifier driving the HSHMD.

In any case, the principle proves its high efficiency. The final damping values with gain $g = 180$ of the two poles are around 24% and 38% (blue squares).

8 Conclusion

This article presents a new control law for hybrid vibration attenuation called hybrid skyHook mass damper. Theoretical analyses, based on a mechanical analogy or a power flow formulation, shows that it enables the synthesis of an active skyhook damper, associated with a passive TMD. With this hybrid device using the TMD as an inertial actuator, the system can be considered as *fail-safe*. The hyperstability property is theoretically ensured, which means that the stability of the controlled system is guaranteed. The performance and robustness have been illustrated through numerical simulations, and an experimental application validates the concept. It was shown that the HSHMD has remarkable properties in term of vibration attenuation on the whole frequency range. Contrary to many hybrid controllers, no response amplifications are observed which appears as its main advantage. Future works will focus on multiple degree of freedom systems and the effect of actuator saturation or non-linearities on the controller.

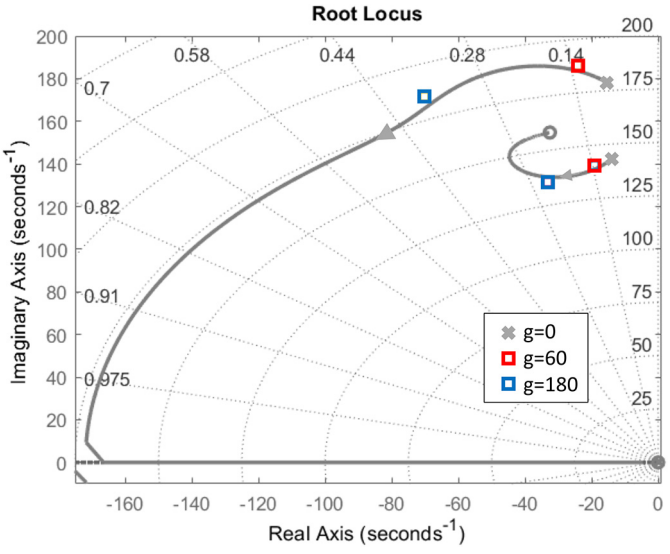

Fig. 12. Root locus of the hybrid controller as a function of the control gain. Square: Experimental results.

References

[1] J. Ormondroyd, J. Den Hartog, The theory of damped vibration absorber, J. Appl. Mech. **50**, 7 (1929)
[2] J. Den Hartog, Mechnical Vibrations, 4th edn., McGraw-Hill, New York, 1956
[3] T. Asami, O. Nishihara, A. Baz, Analytical solutions to H_∞ and H_2 optimization of dynamic vibration absorbers attached to damped linear systems, Trans. ASME **124**, 284 (2002)
[4] I. Jordanov, B. Cheshankov, Optimal design of linear and non-linear dynamic vibration absorbers, J. Sound Vib. **123**, 157–170 (1988)
[5] G. Pennisi, B. Mann, N. Naclerio, C. Stephan, G. Michon, Design and experimental study of a nonlinear energy sink coupled to an electromagnetic energy harvester, J. Sound Vib. **437**, 340–357 (2018)
[6] S. Mahajan, R. Redfield, Power flow in linear, active vibration isolation systems, J. Vib. Acoust. **120**, 571–578 (1998)
[7] J. Rohlfing, S. Elliott, P. Gardonio, Feedback compensator for control units with proof-mass electrodynamic actuators, J. Sound Vibr. **331**, 3437–3450 (2012)

[8] M. Zilletti, Feedback control unit with an inerter proof-mass electrodynamic actuator, J. Sound Vibr. **369**, 16–28 (2016)
[9] S. Camperi, M.G. Tehrani, S.J. Elliott, Parametric study on the optimal tuning of an inertial actuator for vibration control of a plate: theory and experiments, J. Sound Vibr. **435** (2018)
[10] S. Chesné, G. Inquieté, P. Cranga, F. Legrand, B. Petitjean, Innovative hybrid mass damper for dual-loop controller. Mech. Syst. Signal Process. **115**, 514–523 (2019)
[11] R.C. Ümütlü, H. Ozturk, B. Bidikli, A robust adaptive control design for active tuned mass damper systems of multistory buildings, J. Vibr. Control **0**, 1077546320966236 (2020)
[12] L. Huo, G. Song, H. Li, K. Grigoriadis, h_∞ robust control design of active structural vibration suppression using an active mass damper, Smart Mater. Struct. **17**, 015021 (2007)
[13] J. Yuan, Hybrid dynamic vibration absorption by zero/pole placement. ASME J. Vibr. Acoust. **122**, 466–469 (2000)
[14] X. Yan, Z.-D. Xu, Q.-X. Shi, Fuzzy neural network control algorithm for asymmetric building structure with active tuned mass damper. J. Vibr. Control **26**, 2037–2049 (2020)
[15] A. Paknejad, G. Zhao, S. Chesné, A. Deraemaeker, C. Collette, Hybrid electromagnetic shunt damper for vibration control. J. Vibr. Acoust. **143**, 021010 (2021)
[16] G. Paillot, S. Chesné, D. Rémond, Hybrid coupled damper for the mitigation of torsional vibrations and rotational irregularities in an automotive crankshaft: concept and design subtleties, Mech. Based Des. Struct. Mach. **0**, 1–18 (2021)
[17] C. Collette, S. Chesné, Robust hybrid mass damper, J. Sound Vibr. **375** (2016)
[18] S. Chesné C. Collette, Experimental validation of fail-safe hybrid mass damper, J. Vibr. Control, **24**, 4395-4406 (2018)
[19] A. Preumont, Vibration Control of Active Structures An Introduction, 2nd edn., Kluwer Academic Publishers, Dordrecht, The Netherlands, 2002
[20] C. Fuller, A. von Flotow, Active control of sound and vibration. IEEE **0272-1708** (1995)
[21] S. Griffin, J. Gussy, S.A. Lane, B.K. Henderson, D. Sciulli, Virtual skyhook vibration isolation system, J. Vibr. Acoust. **124**, 63–67 (2001)
[22] M. Auleley, O. Thomas, C. Giraud-Audine, H. Mahé, Enhancement of a dynamic vibration absorber by means of an electromagnetic shunt. J. Intell. Mater. Syst. Struct. **32(3)**, 331–354 (2021)
[23] D. Demetris, N. Nikolaos, Hybrid semi-active mass dampers in structures; assessing and optimising their damping capacity, Proc. Eng. **199**, 3103–3108 (2017)
[24] C. Meinhardt, N. Nikitas, D. Demetriou, Application of a 245 metric ton dual-use active TMD system, Proc. Eng. **199**, 1719–1724 (2017)
[25] N. Alujevic, I. Catipovic, S. Malenica, I. Senjanovic, N. Vladimir, Stability, performance and power flow of active u-tube anti-roll tank, Eng. Struct. **211**, 110267 (2020)
[26] J. Rodriguez, P. Cranga, S. Chesne, L. Gaudiller, Hybrid active suspension system of a helicopter main gearbox, J. Vibr. Control **24**, 956–974 (2018)
[27] J. Slotine, W. Li, Applied nonlinear control Englewood Cliffs, Prentice Hall, 1991
[28] D.J. Hartog, Mechanical Vibrations, 4th edn., Mc Graw-Hill, New York, 1956
[29] S. Chesné, C. Collette, Towards low consumption smart dampers. Forum Acusticum, Lyon, France (2020) 195–198
[30] H. Garnier, M. Mensler, A. Richard, Continuous-time model identification from sampled data: implementation issues and performance evaluation, Int. J. Control **76**, 1337–1357 (2003)

Cite this article as: S. Chesné, Hybrid skyhook mass damper, Mechanics & Industry **22**, 49 (2021)